

1 **mRNA-1273 and Ad26.COVS vaccines protect against the B.1.621 variant of**
2 **SARS-CoV-2**

3

4 Tamarand L. Darling^{1,*}, Baoling Ying^{1,*}, Bradley Whitener^{1,*}, Laura A. VanBlargan¹, Traci L.
5 Bricker¹, Chieh-Yu Liang², Astha Joshi¹, Gayan Bamunuarachchi¹, Kuljeet Sehra¹, Aaron J.
6 Schmitz², Peter J. Halfmann⁵, Yoshihiro Kawaoka^{5,6,7}, Sayda M. Elbashir⁸, Darin K. Edwards⁸,
7 Larissa B. Thackray¹, Michael S. Diamond^{§,1,2,3,4}, Adrianus C. M. Boon^{§,1,2,3}.

8

9 ¹ Department of Medicine, ² Department of Pathology and Immunology, and ³ Department of
10 Microbiology, Washington University School of Medicine in St. Louis, MO 63110, USA. ⁴ The
11 Andrew M. and Jane M. Bursky Center for Human Immunology and Immunotherapy Programs,
12 Washington University School of Medicine. St. Louis, MO 63110, USA. ⁵ Department of
13 Pathobiological Sciences, School of Veterinary Medicine, University of Wisconsin, Madison, WI
14 53711. ⁶ Department of Virology, Institute of Medical Science, University of Tokyo, Tokyo 108-
15 8639, Japan. ⁷ The Research Center for Global Viral Diseases, National Center for Global
16 Health and Medicine Research Institute, Tokyo 162-8655, Japan. ⁸ Moderna, Inc., Cambridge,
17 MA 02139, USA.

18

19 * Authors contributed equally

20 § Co-corresponding authors. Adrianus C. M. Boon (jboon@wustl.edu) and Michael S. Diamond
21 (mdiamond@wustl.edu)

22 Lead Contact: Adrianus C. M. Boon

23

24

25 Running Title: COVID-19 vaccines protect against the B.1.621 variant.

26 **ABSTRACT**

27 Since the emergence of severe acute respiratory syndrome coronavirus 2 (SARS-CoV-2) in
28 2019, viral variants with greater transmissibility or immune evasion properties have arisen,
29 which could jeopardize recently deployed vaccine and antibody-based countermeasures. Here,
30 we evaluated in mice and hamsters the efficacy of preclinical non-GMP Moderna mRNA vaccine
31 (mRNA-1273) and the Johnson & Johnson recombinant adenoviral-vectored vaccine
32 (Ad26.COVS.S) against the B.1.621 (Mu) South American variant of SARS-CoV-2, which
33 contains spike mutations T95I, Y144S, Y145N, R346K, E484K, N501Y, D614G, P681H, and
34 D950N. Immunization of 129S2 and K18-human ACE2 transgenic mice with mRNA-1273
35 vaccine protected against weight loss, lung infection, and lung pathology after challenge with
36 B.1.621 or WA1/2020 N501Y/D614G SARS-CoV-2 strain. Similarly, immunization of 129S2
37 mice and Syrian hamsters with a high dose of Ad26.COVS.S reduced lung infection after
38 B.1.621 virus challenge. Thus, immunity induced by mRNA-1273 or Ad26.COVS.S vaccines can
39 protect against the B.1.621 variant of SARS-CoV-2 in multiple animal models.

40 INTRODUCTION

41 Severe acute respiratory syndrome coronavirus 2 (SARS-CoV-2), the etiological agent of
42 coronavirus disease 2019 (COVID-19), has caused hundreds of millions of infections worldwide
43 with more than 5 million deaths. Vaccines targeting the SARS-CoV-2 spike protein were
44 developed within one year of the start of the pandemic. Several of these (mRNA and adenoviral-
45 vectored) are remarkably effective in protecting against severe COVID-19, with efficacy rates
46 ranging from 75 to 95% depending on the vaccine and age of the individual [1-3]. Vaccines also
47 protect against infection, and likely transmission, albeit at lower 50-70% rates [4, 5]. The
48 emergence of several SARS-CoV-2 variants with amino acid substitutions in the spike protein
49 has jeopardized the efficacy of current vaccines to protect against infection and disease. These
50 variants can be more transmissible and also evade serum neutralizing antibodies. As an
51 example, while the Delta variant (B.1.617.2) had no appreciable effect on vaccine efficacy
52 against hospitalization, vaccine-mediated protection against infection was markedly reduced [1-
53 5]. Thus, evaluating vaccine efficacy against emerging variants of SARS-CoV-2 is important for
54 deciding when to administer booster shots, and determining if and when mono- or multivalent
55 vaccines with variant spike antigens are needed.

56 After the emergence of the first D614G variant, several variants of concern (VOC) or interest
57 (VOI) arose including B.1.1.7 (Alpha), B.1.351 (Beta), B.1.1.28 (Gamma), B.1.617.2 (Delta), and
58 more recently B.1.1.529 (Omicron). Isolates from these lineages showed increased resistance
59 to neutralizing antibodies and enhanced transmissibility compared to the antecedent SARS-
60 CoV-2 strains [6-8]. Beyond these major VOC, other variants have emerged. The B.1.621 (Mu)
61 variant was first detected in Colombia in January of 2021, and since then has spread to 51
62 countries including the United States, Japan, and the United Kingdom. The spike protein of
63 B.1.621 varies at nine positions compared to the original SARS-CoV-2 isolate: T38I, Y144T,
64 Y145S, R346K, E484K, N501Y, D614G, P681H, D950N [9]. The E484K mutation, also found in
65 the B.1.351 (Beta) and P.1 (Gamma) variant, is predicted to reduce serum neutralizing antibody

66 titers against this virus. The R346K mutation, first identified in B.1.621, and more recently in a
67 subset of B.1.1.529 (Omicron), is considered a key mutation that confers resistance to serum
68 antibodies from convalescent and vaccinated individuals [10] and class 2 neutralizing
69 monoclonal antibodies (mAbs) [11]. In serum from individuals immunized with Ad26.COVS.S,
70 mRNA-1273 or BNT162b2 vaccines, difference in neutralization comparing historical and
71 B.1.621 SARS-CoV-2 ranged from 2.1-8.7 fold depending on the study population and vaccine
72 [12-16]. A similar difference (4.7-12 fold) in neutralization was observed in convalescent sera
73 from previously infected individuals [13, 14]. However, the impact of the spike mutations in
74 B.1.621 on the protective efficacy of vaccines *in vivo* remains unknown. Here, we evaluated the
75 immunogenicity and efficacy of two vaccines currently under Emergency Use Authorization
76 (EUA), mRNA-1273 (Moderna) and Ad26.COVS.S (Johnson & Johnson), against the B.1.621
77 variant of SARS-CoV-2. We show that immunity induced by mRNA-1273 and Ad26.COVS.S
78 protects mice and hamsters from challenge with the B.1.621 variant of SARS-CoV-2.

79 RESULTS

80 **Immunogenicity and protection by Ad26.COVS2 vaccine against B.1.621 challenge in**
81 **129S2 mice.** Groups of 5-6 week-old male 129S2 mice were immunized once with 10^8 , 10^9 or
82 10^{10} virus particles of the Ad26.COVS2 vaccine (**Fig 1A**). Serum was collected 21 and 115
83 days later, and antibody responses were evaluated by ELISA for spike (S)-specific antibody
84 responses. As expected, serum from control mice that received PBS did not bind to the S
85 protein by ELISA (**Fig 1B**). In comparison, serum collected from mice 115 days after
86 immunization with 10^8 , 10^9 or 10^{10} dose of Ad26.COVS2 contained anti-S specific antibodies
87 with a geometric mean titer (GMT) of 1:21,087, 1:19,870 and 1:80,599 respectively (**Fig 1B**).
88 The serum anti-S antibody response was higher in animals that received 10^{10} dose ($P < 0.001$,
89 **Fig 1B**) than those immunized with 10^8 or 10^9 dose of vaccine. A comparison of the anti-S
90 response between 21 and 115 days after immunization revealed an approximately 3-fold
91 increase in anti-S response over time (**Fig S1C**). Serum samples also were tested for
92 neutralization of SARS-CoV-2 by focus reduction neutralization test (FRNT). Whereas serum
93 from the control animals did not neutralize WA1/2020 N501Y/D614G or B.1.621 (**Fig 1C**), serum
94 from mice immunized with 10^8 , 10^9 , or 10^{10} dose of Ad26.COVS2 did (WA1/2020
95 N501Y/D614G: GMT of 1:3,602, 1:6,071 and 1:20,592, respectively; and B.1.621: GMT of
96 1:3,172, 1:4,460 and 1:20,520, respectively) (**Fig 1C** and **S2A**). No significant difference ($P >$
97 0.5) in serum neutralization was observed between the WA1/2020 N501Y/D614G and B.1.621
98 strains. Also, no significant difference ($P > 0.5$) was observed in a pairwise comparison of
99 serum neutralization titers against WA1/2020 N501Y/D614G and B.1.621 (**Fig S2A**).

100 Next, we challenged the Ad26.COVS2-immunized 129S2 mice with 10^5 plaque forming-
101 units (PFU) of WA1/2020 N501Y/D614G or B.1.621 virus, and 3 days later collected nasal
102 washes and the left lung lobe for viral burden analysis. We used 129S2 mice for these studies
103 because these animals are permissive to infection by some SARS-CoV-2 variants (e.g., B.1.1.7,
104 B.1.1.28, and B.1.351) or mouse-adapted or engineered strains [17-19] that encode an N501Y

105 mutation, which enables engagement of murine ACE2 [20]. Infection of 129S2 mice with SARS-
106 CoV-2 results in mild to moderate lung infection and clinical disease with subsequent recovery
107 [17, 19]. In the nasal wash of control animals challenged with WA1/2020 N501Y/D614G, we
108 detected $\sim 10^5$ copies of the *N* gene transcript per mL (**Fig 1D**). Immunization with 10^8 , 10^9 , or
109 10^{10} dose of Ad26.COVS.S reduced the viral RNA levels by 10, 9 and 8-fold ($P < 0.01$, 0.05, and
110 0.05 respectively, **Fig 1D**). After challenge with B.1.621, we measured $\sim 10^6$ copies of *N* gene
111 transcript per mL in the nasal wash, and this was reduced 3, 8, and 15-fold ($P < 0.01$ for 10^{10}
112 dose) in animals immunized with 10^8 , 10^9 , or 10^{10} dose of Ad26.COVS.S, respectively.

113 Viral RNA levels also were quantified in the left lung lobe at 3 dpi. In the control groups
114 challenged with the WA1/2020 N501Y/D614G virus, $\sim 10^7$ *N* gene transcript copies per mg and
115 $\sim 10^7$ PFU/mL were measured in lung homogenates (**Fig 1E-F**). Immunization with the 10^8 , 10^9 ,
116 or 10^{10} dose of Ad26.COVS.S reduced the *N* gene copy number by 15, 80, and 20,000-fold ($P <$
117 0.05, 0.001, and 0.0001 respectively) and infectious virus levels by 10^3 , 10^5 , and 10^6 -fold ($P =$
118 0.06, < 0.001 , and < 0.0001 , respectively) (**Fig 1E-F**). A second cohort of Ad26.COVS.S-
119 immunized animals were challenged with the B.1.621 strain of SARS-CoV-2. In the control
120 groups, we detected $\sim 10^6$ *N* gene transcript copies per mg and $\sim 10^6$ PFU/mL of infectious virus
121 of lung homogenate (**Fig 1E-F**). Immunization with the 10^8 , 10^9 , or 10^{10} dose of Ad26.COVS.S
122 reduced the viral RNA levels by 18, 30, and 250-fold ($P < 0.01$, 0.01, and 0.0001, respectively)
123 and infectious virus burden by 350, 2,000, and 50,000-fold ($P < 0.05$, 0.01, and 0.0001,
124 respectively) (**Fig 1E-F**).

125 **Immunogenicity and protection by mRNA-1273 against B.1.621 challenge in K18-**
126 **hACE2 mice.** Next, we evaluated the efficacy of preclinical non-GMP lots of the Moderna
127 mRNA-1273 vaccine encoding a sequenced-optimized 2 proline-stabilized spike protein of
128 Wuhan-1 for protection against B.1.621 in K18-hACE2 transgenic mice. Groups of 7-8 week-old
129 female mice were immunized and boosted via intramuscular route with a low (0.25 μ g) or high
130 (5 μ g) dose of the mRNA-1273 or a control mRNA vaccine (mRNA-control, **Fig 2A**). Serum was

131 collected 21 days after the second immunization, and inhibitory antibody responses were
132 evaluated by FRNT against WA1/2020 N501Y/D614G and B.1.621. As expected, serum from
133 mice immunized with the control vaccine did not inhibit virus infection (**Fig 2B**). In contrast,
134 serum from mice immunized with 0.25 μ g dose of mRNA-1273 neutralized infectious virus with
135 GMT of 1:1,125 and 1:434 for WA1/2020 N501Y/D614G and B.1.621 viruses, respectively.
136 Serum from mice immunized with 5 μ g of mRNA-1273 showed greater neutralizing activity
137 against WA1/2020 N501Y/D614G and B.1.621 with GMT of 1:19,751 and 1:15,130 respectively.
138 A statistical difference in serum GMT was observed between WA1/2020 N501Y/D614G and
139 B.1.621 for the low dose ($P < 0.05$), but not the high dose ($P > 0.5$) vaccine. However, a
140 pairwise comparison showed a 1.3 to 2.3-fold difference in serum neutralizing antibody titer
141 between WA1/2020 N501Y/D614G and B.1.621 for the high ($P < 0.05$) and low ($P < 0.01$) dose
142 mRNA-1273 immunized mice (**Fig S2B**).

143 We next evaluated the protective effect of mRNA-1273 vaccine in K18-hACE2 mice. Mice
144 immunized with mRNA-1273 or control mRNA vaccine were challenged via intranasal route with
145 10^3 PFU of WA1/2020 N501Y/D614G or B.1.621 virus, and body weight was recorded for 7
146 days before a nasal wash and the left lung lobe were collected for viral burden analysis. In the
147 control groups challenged with the WA1/2020 N501Y/D614G virus, substantial weight loss was
148 observed at 6 and 7 dpi. Immunization with 0.25 or 5 μ g of mRNA-1273 significantly prevented
149 weight loss ($P < 0.05$ and 0.01 respectively, **Fig 2C**). Similar protection against weight loss after
150 challenge with B.1.621 was observed in the groups immunized with 0.25 ($P = 0.19$) or 5 μ g ($P <$
151 0.05) of mRNA-1273 (**Fig 2D**).

152 We quantified the amount of viral RNA in the nasal wash at 7 dpi. In control vaccinated
153 animals challenged with WA1/2020 N501Y/D614G, we detected $\sim 10^5$ copies of the SARS-CoV-
154 2 *N* gene transcript per mL in the nasal wash (**Fig 2E**). Immunization with mRNA-1273 reduced
155 the levels of WA1/2020 N501Y/D614G RNA by 20 to 45-fold for the 0.25 μ g ($P < 0.05$) and 5 μ g
156 ($P < 0.01$) doses, respectively (**Fig 2E**). In the groups vaccinated with the control mRNA and

157 challenged with the B.1.621 virus, we detected 10^5 - 10^6 copies of the *N* gene transcript per mL in
158 the nasal wash (**Fig 2E**). Immunization with 0.25 μ g ($P = 0.1$) or 5 μ g ($P < 0.001$) of mRNA-1273
159 reduced the *N* gene copy number by ~25 and 200-fold, respectively (**Fig 2E**).

160 The amount of virus in lung homogenates also was quantified. In the control group
161 challenged with WA1/2020 N501Y/D614G, $\sim 10^6$ copies of the *N* transcript per mg and 10^5 - 10^6
162 PFU/g tissue were detected (**Fig 2F-G**). Immunization with 0.25 μ g of mRNA-1273 resulted in
163 markedly reduced ($\sim 20,000$ -fold, $P < 0.0001$) levels of viral RNA and no detectable infectious
164 virus titer in the lung (**Fig 2F-G**). Similar results were seen in mice immunized with 5 μ g of
165 mRNA-1273 (**Fig 2F-G**). A second group of immunized animals were challenged with B.1.621.
166 In the control mRNA vaccinated groups, we detected high levels of viral RNA (*N* gene, $>10^6$
167 copies per mg) and infectious virus (6×10^5 PFU/g) in lung homogenates (**Fig 2F-G**).
168 Immunization with either dose of mRNA-1273 vaccine significantly reduced levels of B.1.621
169 viral RNA and infectious virus in the lung ($\sim 20,000$ -fold, $P < 0.0001$, **Fig 2F-G**).

170 K18-hACE2 mice vaccinated with 0.25 μ g or 5 μ g of mRNA-1273 also had markedly
171 reduced, if not absent, lung pathology at 7 dpi compared to the control mRNA vaccinated and
172 challenged animals (**Fig S3**). Overall, these data indicate that the mRNA-1273 vaccine protects
173 against the B.1.621 variant of SARS-CoV-2 in K18-hACE2 mice.

174 **Immunogenicity and protection by mRNA-1273 vaccine against B.1.621 challenge in**
175 **129S2 mice.** To corroborate our findings, we also tested the mRNA-1273 vaccine in
176 immunocompetent 129S2 mice. Groups of 7-8 week-old female mice were immunized and
177 boosted via intramuscular route with 0.25 or 5 μ g of mRNA-1273 or control mRNA vaccine (**Fig**
178 **3A**). Serum was collected 21 days after the second immunization, and antibody responses were
179 evaluated by FRNT. As expected, serum from 129S2 mice immunized with the control mRNA
180 vaccine did not neutralize virus infection (**Fig 3B**). In contrast, serum from mice immunized with
181 5 μ g of mRNA-1273 robustly neutralized infection with GMTs of 1:40,066 and 1:38,675 for
182 WA1/2020 N501Y/D614G and B.1.621, respectively. Sera from mice immunized with the 0.25

183 μg dose of mRNA-1273 inhibited infection of WA1/2020 N501Y/D614G and B.1.621 to a lesser
184 extent with GMTs of 1:2,665 and 1:2,407, respectively. No significant difference ($P > 0.5$) in
185 vaccine-induced GMTs were observed between the WA1/2020 N501Y/D614G and B.1.621
186 viruses (**Fig 3B**). Also no significant difference ($P > 0.5$) was observed in a pairwise comparison
187 of the neutralization titer against WA1/2020 N501Y/D614G and B.1.621 in serum from 129S2
188 mice immunized with high and low dose mRNA-1273 vaccine (**Fig S2C**).

189 We next challenged immunized 129S2 mice with 10^5 PFU of WA1/2020 N501Y/D614G or
190 B.1.621 via an intranasal route. Weights were recorded for 4 days before the animals were
191 sacrificed, and nasal washes and the left lung lobe were collected for viral burden analysis.
192 Control animals challenged with the WA1/2020 N501Y/D614G virus lost ~10% of their starting
193 body weight by 4 dpi (**Fig 3C**). Immunization with 0.25 and 5 μg of mRNA-1273 reduced the
194 weight loss ($P < 0.001$ and 0.01 respectively, **Fig 3C**). Inoculation of control-vaccinated 129S2
195 mice with B.1.621 resulted in ~7% weight loss at 4 dpi (**Fig 3D**), and immunization with 0.25 or
196 5 μg of mRNA-1273 prevented this weight loss ($P < 0.05$).

197 In animals vaccinated with the control mRNA and challenged with the WA1/2020
198 N501Y/D614G virus, we detected $\sim 10^6$ copies/mL of *N* gene transcript (**Fig 3E**) in the nasal
199 wash at 4 dpi. Immunization with 0.25 or 5 μg of mRNA-1273 reduced WA1/2020
200 N501Y/D614G viral RNA levels in the nasal wash (~200-fold, $P < 0.001$). In mice vaccinated
201 with the control mRNA vaccine and challenged with B.1.621, we detected $\sim 10^6$ *N* gene
202 transcript copies per mL in the nasal wash (**Fig 3E**). Immunization with 0.25 μg or 5 μg of
203 mRNA-1273 reduced the viral RNA levels substantially (~200-fold, $P < 0.001$; **Fig 3E**). Viral
204 burden also was measured in lung homogenates of these same animals. In the control mRNA
205 group challenged with the WA1/2020 N501Y/D614G virus, we detected $\sim 10^8$ copies/mg of *N*
206 gene transcript (**Fig 3F**) and $> 10^6$ PFU/g of infectious virus (**Fig 3G**) in lung homogenates.
207 Immunization with 0.25 μg of mRNA-1273 effectively reduced the viral RNA (10^6 -fold, $P < 0.001$,
208 **Fig 3F**) and infectious virus levels (1,000-fold, $P < 0.001$, **Fig 3G**), although some animals

209 showed breakthrough infection. Immunization with 5 µg dose of mRNA-1273 also reduced the
210 levels of viral RNA (10^6 -fold, $P < 0.001$) and infectious virus (1,000-fold, $P < 0.001$, **Fig 3F-G**).
211 Importantly, no breakthrough infection was detected. A second group of immunized animals
212 were challenged with the B.1.621 virus. In the control mRNA vaccinated groups, we detected in
213 the lung homogenates $\sim 10^7$ copies/mg of viral RNA transcript (**Fig 3F**) and $\sim 10^6$ PFU/g of
214 infectious virus (**Fig 3E**). Immunization with 0.25 or 5 µg doses of mRNA-1273 significantly
215 reduced B.1.621 viral RNA (10^5 -fold, $P < 0.0001$) and infectious virus (1,000-fold, $P < 0.0001$)
216 levels in the lung (**Fig 3F-G**) to a similar degree after WA1/2020 N501Y/D614G challenge.

217 The reduction in viral burden in the lungs of mice immunized with 0.25 or 5 µg of mRNA-
218 1273 and challenged with WA1/2020 N501Y/D614G or B.1.621 corresponded with an absence
219 of lung pathology at 4 dpi (**Fig S4**). Lung sections from mice immunized with a control mRNA
220 and challenged with WA1/2020 N501Y/D614G or B.1.621 showed evidence of immune cell
221 infiltration and tissue damage. Immunization with 0.25 and 5 µg of mRNA-1273 prevented the
222 lung pathology after challenge with both WA1/2020 N501Y/D614G and B.1.621 virus. Overall,
223 these data indicate that the mRNA-1273 vaccine protects against the B.1.621 variant of SARS-
224 CoV-2 in non-transgenic immunocompetent 129S2 mice.

225 **Immunogenicity and protection by Ad26.COVS vaccine against B.1.621 challenge in**
226 **Syrian hamsters.** We next evaluated the efficacy of a single dose of the Ad26.COVS vaccine
227 in Syrian hamsters. Syrian hamsters are naturally susceptible to SARS-CoV-2 and considered
228 an excellent model for COVID-19 [19, 21-24]. Groups of 5-6 week-old male hamsters were
229 immunized once with 10^8 or 10^{10} dose of the Ad26.COVS vaccine (**Fig 4A**). Serum was
230 collected 21 days later, and antibody responses were evaluated by ELISA and FRNT. As
231 expected, serum from control hamsters that received PBS did not bind viral S protein (**Fig 4B**).
232 However, sera collected from hamsters immunized with 10^8 or 10^{10} dose of Ad26.COVS
233 contained anti-S antibodies with GMTs of 1:7,506, and 1:40,913 respectively (**Fig 4B**). The
234 serum anti-S antibody response was higher in animals receiving the 10^{10} vaccine dose ($P <$

235 0.05, **Fig 4B**). Serum samples were tested for neutralization of SARS-CoV-2 by FRNT. Serum
236 from hamsters immunized with 10^8 or 10^{10} dose of Ad26.COVS neutralized WA1/2020 with
237 GMT of 1:381 and 1:1,692 respectively (**Fig 4C**), and B.1.621 with GMT of 1:136 and 1:501,
238 respectively (**Fig 4C**). No difference in GMT was observed with respect to neutralization of
239 WA1/2020 and B.1.621 variant after immunization with 10^8 ($P = 0.06$) or 10^{10} ($P = 0.6$) dose of
240 Ad26.COVS (**Fig 4C**). A pair-wise comparison found a ~3-fold reduction in serum neutralizing
241 antibody titer between WA1/2020 and B.1.621 for the high ($P < 0.0001$) and low ($P < 0.001$)
242 dose Ad26-COVS immunized hamsters (**Fig S2D**).

243 Seventy days after immunization, the hamsters were challenged via an intranasal route with
244 10^3 PFU of WA1/2020 or B.1.621. Four days later, the animals were sacrificed, and a nasal
245 wash and the left lung lobe were collected for viral burden analysis. In the nasal wash of control
246 animals challenged with the WA1/2020 virus, we detected $\sim 10^6$ copies of the *N* gene transcript
247 per mL of nasal wash (**Fig 4D**) and $\sim 10^4$ PFU/mL of infectious virus (**Fig 4E**). Immunization with
248 10^8 or 10^{10} dose of Ad26.COVS did not reduce the viral RNA levels in the nasal wash (**Fig**
249 **4D**), although the infectious virus titer was decreased by 16 and 46-fold ($P > 0.05$ and < 0.05
250 respectively, **Fig 4E**). Upon challenge of hamsters with B.1.621, we detected $\sim 10^6$ *N* gene
251 copies per mL (**Fig 4D**) and $\sim 10^3$ PFU/mL of infectious virus (**Fig 4E**) in the nasal wash.
252 Immunization with 10^8 or 10^{10} dose of Ad26.COVS reduced the *N* gene copy number 19-fold (P
253 > 0.05 , **Fig 4D**). In comparison, the infectious virus titer was reduced by 2 and 17-fold ($P > 0.05$
254 and < 0.05 for 10^8 and 10^{10} dose respectively, **Fig 4E**)

255 We also measured the viral burden in lung homogenates of hamsters. In the control group
256 challenged with WA1/2020, the *N* gene copy number was $\sim 10^7$ copies per mg (**Fig 4F**) and the
257 infectious virus levels were $\sim 10^7$ PFU/mL (**Fig 4G**). Immunization with the 10^8 or 10^{10} dose of
258 Ad26.COVS reduced the viral RNA (11 and 360-fold, $P > 0.05$ and < 0.01) and infectious virus
259 (66 and 4800-fold, $P = 0.06$ and < 0.001) levels (**Fig 4F-G**). After B.1.621 challenge of the
260 control group, we detected $\sim 10^7$ *N* gene copies per mg of tissue (**Fig 4F**) and $\sim 10^7$ PFU/mL of

261 infectious virus in the lung (**Fig 4G**). Immunization with the 10^8 or 10^{10} dose of Ad26.COVS
262 reduced the viral RNA (7 and 540-fold, $P > 0.05$ and < 0.05) and infectious virus (100 and
263 25,500-fold, $P = 0.13$ and < 0.001) levels (**Fig 4F-G**).

264 DISCUSSION

265 In this study, we evaluated the efficacy of two vaccines under EUA, mRNA-1273 and
266 Ad26.COVS2, against the B.1.621 variant of SARS-CoV-2 in in three pre-clinical models;
267 129S2-immuno-competed mice, K18-hACE2 transgenic mice, and Syrian hamster. The mRNA-
268 1273 vaccine induced high levels of neutralizing antibodies against WA1/2020 N501Y/D614G
269 and B.1.621 viruses, and this response was associated with robust protection from an intranasal
270 challenge. Immunization of 129S2 mice or Syrian hamsters with different doses of
271 Ad26.COVS2 induced moderate to high serum neutralizing antibody responses against the
272 B.1.621 virus. However, only the high dose (10^{10} virus particles) Ad26.COVS2 reduced virus
273 titers substantially.

274 Our studies provide a comparison of the immunogenicity and efficacy of the Ad26.COVS2
275 and mRNA-1273 vaccines in 129S2 mice. The serum neutralizing antibody titer was similar after
276 one dose of Ad26.COVS2 or two doses of mRNA-1273 in 129S2 mice, and this was true for
277 both the high dose (5 μ g vs. 10^{10} virus particles) and the low dose (0.25 μ g vs. 10^8 virus
278 particles) vaccine regimen. Despite the similarity in neutralization titer, the mRNA-1273 vaccine
279 more effectively reduced viral load in the lungs of WA1/2020 N501Y/D614G or B.1.621
280 challenged animals than the Ad26.COVS2 vaccine. In mice immunized with a low-dose of the
281 mRNA-1273 vaccine, approximately 20% of the animals showed evidence of breakthrough
282 infections after challenge (**Fig 3G**). In contrast, 75% of the animals that received a low dose of
283 Ad26.COVS2 and were challenged with WA1/2020 N501Y/D614G or B.1.621 showed virus
284 breakthrough despite relatively equivalent levels of serum neutralizing antibodies titers at the
285 time of challenge (**Fig 1F**). One explanation for this difference could be that the mRNA vaccine
286 requires two doses, while the Ad26.COVS2 vaccine was only given once. Another possibility is
287 the time between the last immunization and the virus challenge, which is 41 and 115 days for
288 the mRNA-1273 and Ad26.COVS2 immunized animals, respectively. Differences in the
289 glycosylation pattern or the IgG subclass of antibodies between anti-S antibodies induced by

290 mRNA-1273 and Ad26.COVS induced could contribute to differences in protection, as seen in
291 non-human primates and humans [25, 26]. It is also possible that mRNA-1273 vaccine induced
292 a better anamnestic B or T cell response in 129S2 mice compared to the Ad26.COVS vaccine
293 at the time of virus challenge.

294 The antibody response after vaccination varied between the mouse and hamster models.
295 Immunization of mice with 5 µg of mRNA-1273 or 10¹⁰ Ad26.COVS induced serum
296 neutralizing antibody responses with a GMT of > 10,000 in both 129S2 and K18-hACE2 mice. In
297 contrast, in Syrian hamsters, the GMT against WA1/2020 was ~10-fold lower than in mice, yet
298 still several fold higher than that observed in humans vaccinated with one dose of Ad26.COVS
299 [27-30]. The reason for this difference in vaccine response between mice and hamsters
300 remains unknown. It is possible that the hamster immune response targets different epitopes on
301 the spike protein. Alternatively, the spike protein contains fewer T cell epitopes for hamsters
302 compared to the mouse, although that seems unlikely given the size of the antigen. The Syrian
303 hamster also may be a more tolerogenic, perhaps due to its complex microbiome as opposed to
304 the SPF microbiome of 129S2 and K18 TG mice. Mice that received the microbiome from pet
305 stores or from field mice had blunted vaccine responses compared to laboratory-housed mice in
306 pathogen-free facilities [31]. Additional studies are required to elucidate the causes for this
307 difference, but in general, the magnitude of antibody response in Syrian hamsters is more
308 similar to the human antibody response after vaccination.

309 The B.1.621 (Mu) variant of SARS-CoV-2 has R346K and E484K mutations in the receptor
310 binding domain of the spike protein and is believed to be more resistant to virus neutralization
311 by serum antibodies compared to the historical SARS-CoV-2 virus. In sera from vaccinated or
312 infected individuals, the fold difference in neutralization between the D614G (B.1) variant of
313 SARS-CoV-2 and B.1.621 was between 2 and 12-fold [12-16, 32]. In Syrian hamsters, we
314 observed a ~3-fold decrease ($P < 0.001$) in serum neutralization titer between the WA1/2020
315 and B.1.621 virus. In K18-hACE2 mice immunized with mRNA-1273 the difference in serum

316 neutralization titer between WA1/2020 N501Y/D614G and B.1.621 was 1.3 to 2.3-fold. In
317 contrast, no difference in neutralization titer between WA1/2020 N501Y/D614G and B.1.621
318 was observed in 129S2 mice immunized with mRNA-1273 or Ad26.COV2.S, suggesting that
319 mouse strain and species-specific differences in the antibody response. Another reason may be
320 the N501Y mutation in WA1/2020 N501Y/D614G, which has been shown to reduce the
321 neutralization titer of serum and certain monoclonal antibodies compared to WA1/2020 and
322 WA1/2020 D614G, respectively [6, 33]. We used the WA1/2020 N501Y/D614G virus because
323 the N501Y mutation was required for virus infection in immunocompetent 129S2 mice lacking
324 hACE2 expression. Finally, it is possible that the insertion of a threonine at position 144-145 in
325 our particular B.1.621 isolate reduced the resistance to serum neutralizing antibodies.

326 We observed no difference in efficacy of the mRNA and adenoviral-vectored vaccine to
327 protect against B.1.621 in three different animal models. Near full protection, defined by
328 undetectable levels of SARS-CoV-2 viral RNA and infectious virus, plus the absence of
329 immunopathology in the vaccinated animals, was observed against both B.1.621 and the control
330 WA1/2020 virus in mice immunized with mRNA-1273. While immunization with lower doses of
331 Ad26.COV2.S offered only partial protection, we did not observe a difference in virus titer or
332 frequency of breakthrough infection between B.1.621 and control virus. This suggests that a 2-
333 3-fold reduction in serum neutralization titer has limited impact on mRNA and adenoviral
334 vaccine protection against the variant B.1.621 virus.

335 **Limitations of the study.** We note several limitations of our study. (a) We did not evaluate
336 the effects of the vaccine on the transmission of SARS-CoV-2 in Syrian hamsters, which may be
337 an important measure of vaccine protection. (b) We used lower doses of vaccine to mimic
338 suboptimal and possibly waning immunity. Studies that directly compare the quality of a waning
339 immune response to that of a low dose vaccine induced immune response are needed. (c) The
340 challenge dose of SARS-CoV-2 used in our hamster model (10^3 PFU) is several orders of
341 magnitude higher than the minimal infectious dose (5 PFU) [34]. While this creates a very robust

342 virus challenge model, it could underestimate the protective effects of vaccines. (d) We did not
343 establish correlates of immune protection. We noted that lower serum antibody neutralization
344 titers were associated with high viral loads and infectious virus titers in the Ad26.COV2.S
345 immunized animals, as well as breakthrough infections in some of the mRNA-1273 vaccinated
346 mice, albeit this did not explain all breakthrough infections. A more detailed analysis of T cell
347 and non-neutralizing antibody responses coupled with even lower vaccine doses may be
348 needed to fully establish a correlate of protection against breakthrough infection.

349 Overall, our studies demonstrate that the Moderna mRNA-1273 and Johnson & Johnson
350 Ad26.COV2.S vaccines authorized for emergency use are immunogenic in mice and Syrian
351 hamsters and protect against the B.1.621 (Mu) variant of SARS-CoV-2 without substantial loss
352 of potency.

353 REFERENCES

- 354 1. Bajema, K.L., et al., *Effectiveness of COVID-19 mRNA Vaccines Against COVID-19-*
355 *Associated Hospitalization - Five Veterans Affairs Medical Centers, United States,*
356 *February 1-August 6, 2021.* MMWR Morb Mortal Wkly Rep, 2021. **70**(37): p. 1294-1299.
- 357 2. Grannis, S.J., et al., *Interim Estimates of COVID-19 Vaccine Effectiveness Against*
358 *COVID-19-Associated Emergency Department or Urgent Care Clinic Encounters and*
359 *Hospitalizations Among Adults During SARS-CoV-2 B.1.617.2 (Delta) Variant*
360 *Predominance - Nine States, June-August 2021.* MMWR Morb Mortal Wkly Rep, 2021.
361 **70**(37): p. 1291-1293.
- 362 3. Tenforde, M.W., et al., *Sustained Effectiveness of Pfizer-BioNTech and Moderna*
363 *Vaccines Against COVID-19 Associated Hospitalizations Among Adults - United States,*
364 *March-July 2021.* MMWR Morb Mortal Wkly Rep, 2021. **70**(34): p. 1156-1162.
- 365 4. Fowlkes, A., et al., *Effectiveness of COVID-19 Vaccines in Preventing SARS-CoV-2*
366 *Infection Among Frontline Workers Before and During B.1.617.2 (Delta) Variant*
367 *Predominance - Eight U.S. Locations, December 2020-August 2021.* MMWR Morb
368 Mortal Wkly Rep, 2021. **70**(34): p. 1167-1169.
- 369 5. Nanduri, S., et al., *Effectiveness of Pfizer-BioNTech and Moderna Vaccines in*
370 *Preventing SARS-CoV-2 Infection Among Nursing Home Residents Before and During*
371 *Widespread Circulation of the SARS-CoV-2 B.1.617.2 (Delta) Variant - National*
372 *Healthcare Safety Network, March 1-August 1, 2021.* MMWR Morb Mortal Wkly Rep,
373 2021. **70**(34): p. 1163-1166.
- 374 6. Chen, R.E., et al., *Resistance of SARS-CoV-2 variants to neutralization by monoclonal*
375 *and serum-derived polyclonal antibodies.* Nat Med, 2021.
- 376 7. Plante, J.A., et al., *Spike mutation D614G alters SARS-CoV-2 fitness.* Nature, 2021.
377 **592**(7852): p. 116-121.
- 378 8. Liu, Y., et al., *The N501Y spike substitution enhances SARS-CoV-2 infection and*
379 *transmission.* Nature, 2021.
- 380 9. Laiton-Donato, K., et al., *Characterization of the emerging B.1.621 variant of interest of*
381 *SARS-CoV-2.* Infect Genet Evol, 2021. **95**: p. 105038.
- 382 10. Schmidt, F., et al., *High genetic barrier to SARS-CoV-2 polyclonal neutralizing antibody*
383 *escape.* Nature, 2021.
- 384 11. Fratev, F., *The R346K Mutation in the μ Variant of SARS-CoV-2 Alter the*
385 *Interactions with Monoclonal Antibodies from Class 2: A Free Energy of Perturbation*
386 *Study.* bioRxiv, 2021: p. 2021.10.12.463781.
- 387 12. Suthar, M.S., et al., *Durability of immune responses to the BNT162b2 mRNA vaccine.*
388 bioRxiv, 2021: p. 2021.09.30.462488.
- 389 13. Tada, T., et al., *Neutralization of Mu and C.1.2 SARS-CoV-2 Variants by Vaccine-elicited*
390 *Antibodies in Individuals With and Without Previous History of Infection.* bioRxiv, 2021:
391 p. 2021.10.19.463727.
- 392 14. Uriu, K., et al., *Ineffective neutralization of the SARS-CoV-2 Mu variant by convalescent*
393 *and vaccine sera.* bioRxiv, 2021: p. 2021.09.06.459005.
- 394 15. Wang, L., et al., *Differential neutralization and inhibition of SARS-CoV-2 variants by*
395 *antibodies elicited by COVID-19 mRNA vaccines.* bioRxiv, 2021: p. 2021.11.24.469906.
- 396 16. Messali, S., et al., *A cluster of the new SARS-CoV-2 B.1.621 lineage in Italy and*
397 *sensitivity of the viral isolate to the BNT162b2 vaccine.* J Med Virol, 2021. **93**(12): p.
398 6468-6470.
- 399 17. Rathnasinghe, R., et al., *The N501Y mutation in SARS-CoV-2 spike leads to morbidity in*
400 *obese and aged mice and is neutralized by convalescent and post-vaccination human*
401 *sera.* medRxiv, 2021.

- 402 18. Gu, H., et al., *Adaptation of SARS-CoV-2 in BALB/c mice for testing vaccine efficacy.*
403 Science, 2020. **369**(6511): p. 1603-1607.
- 404 19. Chen, R.E., et al., *In vivo monoclonal antibody efficacy against SARS-CoV-2 variant*
405 *strains.* Nature, 2021. **596**(7870): p. 103-108.
- 406 20. Liu, Y., et al., *Functional and genetic analysis of viral receptor ACE2 orthologs reveals a*
407 *broad potential host range of SARS-CoV-2.* Proc Natl Acad Sci U S A, 2021. **118**(12).
- 408 21. Bricker, T.L., et al., *A single intranasal or intramuscular immunization with chimpanzee*
409 *adenovirus-vectored SARS-CoV-2 vaccine protects against pneumonia in hamsters.* Cell
410 Rep, 2021. **36**(3): p. 109400.
- 411 22. Schmitz, A.J., et al., *A vaccine-induced public antibody protects against SARS-CoV-2*
412 *and emerging variants.* Immunity, 2021. **54**(9): p. 2159-2166.e6.
- 413 23. Sia, S.F., et al., *Pathogenesis and transmission of SARS-CoV-2 in golden hamsters.*
414 Nature, 2020.
- 415 24. Su, W., et al., *Neutralizing Monoclonal Antibodies That Target the Spike Receptor*
416 *Binding Domain Confer Fc Receptor-Independent Protection against SARS-CoV-2*
417 *Infection in Syrian Hamsters.* mBio, 2021: p. e0239521.
- 418 25. Gorman, M.J., et al., *Fab and Fc contribute to maximal protection against SARS-CoV-2*
419 *following NVX-CoV2373 subunit vaccine with Matrix-M vaccination.* Cell Rep Med, 2021.
420 **2**(9): p. 100405.
- 421 26. Zohar, T., et al., *Compromised Humoral Functional Evolution Tracks with SARS-CoV-2*
422 *Mortality.* Cell, 2020. **183**(6): p. 1508-1519.e12.
- 423 27. Bos, R., et al., *Ad26 vector-based COVID-19 vaccine encoding a prefusion-stabilized*
424 *SARS-CoV-2 Spike immunogen induces potent humoral and cellular immune responses.*
425 NPJ Vaccines, 2020. **5**: p. 91.
- 426 28. Alter, G., et al., *Immunogenicity of Ad26.COV2.S vaccine against SARS-CoV-2 variants*
427 *in humans.* Nature, 2021. **596**(7871): p. 268-272.
- 428 29. Sadoff, J., et al., *Interim Results of a Phase 1-2a Trial of Ad26.COV2.S Covid-19*
429 *Vaccine.* N Engl J Med, 2021. **384**(19): p. 1824-1835.
- 430 30. Stephenson, K.E., et al., *Immunogenicity of the Ad26.COV2.S Vaccine for COVID-19.*
431 Jama, 2021. **325**(15): p. 1535-1544.
- 432 31. Fiege, J.K., et al., *Mice with diverse microbial exposure histories as a model for*
433 *preclinical vaccine testing.* Cell Host Microbe, 2021.
- 434 32. Miyakawa, K., et al., *Neutralizing efficacy of vaccines against the SARS-CoV-2 Mu*
435 *variant.* medRxiv, 2021: p. 2021.09.23.21264014.
- 436 33. Wang, Z., et al., *mRNA vaccine-elicited antibodies to SARS-CoV-2 and circulating*
437 *variants.* Nature, 2021. **592**(7855): p. 616-622.
- 438 34. Rosenke, K., et al., *Defining the Syrian hamster as a highly susceptible preclinical model*
439 *for SARS-CoV-2 infection.* Emerg Microbes Infect, 2020. **9**(1): p. 2673-2684.
- 440 35. Zang, R., et al., *TMPRSS2 and TMPRSS4 promote SARS-CoV-2 infection of human*
441 *small intestinal enterocytes.* Sci Immunol, 2020. **5**(47).
- 442 36. Nelson, J., et al., *Impact of mRNA chemistry and manufacturing process on innate*
443 *immune activation.* Sci Adv, 2020. **6**(26): p. eaaz6893.
- 444 37. Hassett, K.J., et al., *Optimization of Lipid Nanoparticles for Intramuscular Administration*
445 *of mRNA Vaccines.* Mol Ther Nucleic Acids, 2019. **15**: p. 1-11.
- 446 38. Stadlbauer, D., et al., *SARS-CoV-2 Seroconversion in Humans: A Detailed Protocol for a*
447 *Serological Assay, Antigen Production, and Test Setup.* Curr Protoc Microbiol, 2020.
448 **57**(1): p. e100.
- 449 39. Amanat, F., et al., *A serological assay to detect SARS-CoV-2 seroconversion in*
450 *humans.* Nat Med, 2020. **26**(7): p. 1033-1036.
- 451 40. Liu, Z., et al., *Identification of SARS-CoV-2 spike mutations that attenuate monoclonal*
452 *and serum antibody neutralization.* Cell Host Microbe, 2021. **29**(3): p. 477-488.e4.

- 453 41. Chu, D.K.W., et al., *Molecular Diagnosis of a Novel Coronavirus (2019-nCoV) Causing*
454 *an Outbreak of Pneumonia*. Clin Chem, 2020.
455

456 **ACKNOWLEDGEMENTS**

457 We thank Florian Krammer and Ali Ellebedy for the plasmid and recombinant S protein
458 respectively. This study was supported by the NIH (R01 AI157155, U01 AI151810, NIAID
459 Centers of Excellence for Influenza Research and Response (CEIRR) contract
460 75N93021C00014 and 75N93021C00016, and the Collaborative Influenza Vaccine Innovation
461 Centers (CIVIC) contract 75N93019C00051). It was also supported, in part, by the National
462 Institutes of Allergy and Infectious Diseases Center for Research on Influenza Pathogenesis
463 (HHSN272201400008C), and the Japan Program for Infectious Diseases Research and
464 Infrastructure (JP21wm0125002) from the Japan Agency for Medical Research and
465 Development (AMED).

466

467 **AUTHOR CONTRIBUTIONS**

468 T.L.B., B.Y., B.W., C-Y.L., L.A.V., G.B., and T.L.D. performed mouse and hamster
469 experiments. T.L.B., B.Y., and T.L.D. quantified virus titers in collected tissues. K.S., A.J., and
470 B.W. determined viral load by real-time quantitative RT-PCR. Y.K. and P.J.H. isolated,
471 expanded and sequenced the B.1.621 virus. T.L.D. and L.A.V. performed the virus
472 neutralization assays. M.S.D., A.C.M.B., T.L.D. L.B.T. and B.Y. analyzed the data. A.C.M.B.,
473 and M.S.D. wrote the manuscript, and all authors edited the final version.

474

475 **DECLARATION OF INTERESTS**

476 The Boon laboratory has received unrelated funding support in sponsored research
477 agreements from AI Therapeutics, GreenLight Biosciences Inc., and Nano targeting & Therapy
478 Biopharma Inc. The Boon laboratory has received funding support from AbbVie Inc., for the
479 commercial development of SARS-CoV-2 mAb. M.S.D. is a consultant for Inbios, Vir
480 Biotechnology, Senda Biosciences, and Carnival Corporation, and on the Scientific Advisory

481 Boards of Moderna and Immunome. The Diamond laboratory has received unrelated funding
482 support in sponsored research agreements from Vir Biotechnology, Kaleido, and Emergent
483 BioSolutions and past support from Moderna not related to these studies. S.E. and D.K.E. are
484 employees of and shareholders in Moderna Inc.

485 **FIGURE LEGENDS**

486 **Figure 1. Ad26.COV2.S vaccine protects 129S2 mice against challenge with**
487 **WA1/2020 N501Y/D614G and B.1.621. (A)** Experimental setup. **(B)** Serum anti-S protein
488 antibody response (EC_{50}) in control mice (black symbols), and mice immunized with 10^8 (red
489 symbols), 10^9 (purple symbols), or 10^{10} (blue symbols) of Ad26.COV2.S (**** $P < 0.0001$, *** $P <$
490 0.001 by non-parametric one-way ANOVA with a Dunn's post-test). **(C)** Serum neutralizing titer
491 (IC_{50}) against WA1/2020 N501Y/D614G (circles) or B.1.621 (triangles) measured by FRNT from
492 129S2 mice immunized once with 10^8 (red symbols), 10^9 (purple symbols), or 10^{10} (blue
493 symbols) of Ad26.COV2.S (**** $P < 0.0001$, *** $P < 0.001$, ns = not significant by non-parametric
494 one-way ANOVA with a Dunn's post-test). **(D-F)** 129S2 mice were challenged with 10^5 PFU of
495 the WA1/2020 N501Y/D614G (circles) or B.1.621 (triangles) variant of SARS-CoV-2, and nasal
496 washes **(D)** and lungs **(E-F)** were collected for analysis of viral RNA levels by RT-qPCR **(D)** and
497 infectious virus by plaque assay **(E-F)** (**** $P < 0.0001$, *** $P < 0.001$, ** $P < 0.01$, * $P < 0.05$, ns
498 = not significant by one-way ANOVA with a Dunnett's **(D-E)** or Dunn's **(F)** post-test). **(B-G)** Bars
499 indicate the geometric mean values, and dotted lines are the LOD of the assays. The results are
500 from two independent experiments, and each symbol represents an individual animals.

501 **Figure 2. mRNA-1273 protects K18-hACE2 transgenic mice against challenge with**
502 **N501Y/D614G and B.1.621. (A)** Experimental setup. **(B)** Serum neutralizing titer (IC_{50}) against
503 WA1/2020 N501Y/D614G (red circles) or B.1.621 (blue triangles) from K18-hACE2 mice
504 immunized twice with $0.25 \mu\text{g}$ (open symbols) or $5 \mu\text{g}$ (closed symbols) of mRNA-1273 or
505 mRNA control vaccine (*** $P < 0.001$, **** $P < 0.0001$ by non-parametric one-way ANOVA with
506 a Dunn's post-test). **(C-D)** Mean \pm SEM of weight loss/gain in SARS-CoV-2 challenged mice (**
507 $P < 0.01$, * $P < 0.05$, ns = not significant by two-way ANOVA). **(E-G)** K18-hACE2 mice were
508 challenged with 10^3 PFU of the WA1/2020 N501Y/D614G (red circles) or B.1.621 (blue
509 triangles), and nasal washes **(E)** and lungs **(F-G)** were collected for analysis of viral RNA levels
510 by RT-qPCR **(E)** and infectious virus by plaque assay **(F-G)** (**** $P < 0.0001$, *** $P < 0.001$, ** P

511 < 0.01, * $P < 0.05$, ns = not significant by Mann-Whitney test). (B, E-G) Bars indicate the
512 geometric mean values, and dotted lines are the LOD of the assays. The results are from two
513 independent experiments, and each symbol represents an individual animals.

514 **Figure 3. mRNA-1273 protects 129S2 mice against challenge with WA1/2020**
515 **N501Y/D614G and B.1.621.** (A) Experimental setup. (B) Serum neutralizing titer (IC_{50}) against
516 WA1/2020 N501Y/D614G (red circles) or B.1.621 (blue triangles) from 129S2 mice immunized
517 twice with 0.25 μ g (open symbols) or 5 μ g (closed symbols) of mRNA-1273 or mRNA control
518 vaccine. (**** $P < 0.0001$, *** $P < 0.001$ by non-parametric one-way ANOVA with a Dunn's post-
519 test). (C-D) Mean \pm SEM of weight loss/gain in SARS-CoV-2 challenged mice (** $P < 0.01$, * $P <$
520 0.05, ns = not significant by two-way ANOVA). (E-G) 129S2 mice were challenged with 10^5 PFU
521 of WA1/2020 N501Y/D614G (red symbols) or B.1.621 (blue symbols), and nasal washes (E)
522 and lungs (F-G) were evaluated for viral RNA levels by RT-qPCR (E) and infectious virus by
523 plaque assay (F-G) (**** $P < 0.0001$, *** $P < 0.001$, ** $P < 0.01$, * $P < 0.05$, ns = not significant
524 by Mann-Whitney test). (B, E-G) Bars indicate the geometric mean values, and dotted lines are
525 the LOD of the assays. The results are from two independent experiments, and each symbol
526 represents an individual animals.

527 **Figure 4. Ad26.COVS vaccine protects Syrian hamsters against challenge with**
528 **WA1/2020 and B.1.621.** (A) Experimental setup. (B) Serum anti-S protein antibody response
529 (EC_{50}) in control hamsters (black symbols), and hamsters immunized with 10^8 (red symbols) or
530 10^{10} (blue symbols) of Ad26.COVS (**** $P < 0.0001$, *** $P < 0.001$, ns = not significant by non-
531 parametric one-way ANOVA with a Dunn's post-test. (C) Serum neutralizing titer (IC_{50}) against
532 WA1/2020 (circles) or B.1.621 (triangles) from hamsters immunized once with 10^8 (red symbols)
533 or 10^{10} (blue symbols) of Ad26.COVS (**** $P < 0.0001$, *** $P < 0.001$, ns = not significant by
534 non-parametric one-way ANOVA with a Dunn's post-test. (D-G) Syrian hamsters were
535 challenged with 10^3 PFU of the WA1/2020 (circles) or B.1.621 (triangles), and nasal washes (D-

536 **E**) and lungs (**F-G**) were evaluated for viral RNA levels by RT-qPCR (**D** and **F**) and infectious
537 virus by plaque assay (**E** and **G**) (**** $P < 0.0001$, *** $P < 0.001$, ** $P < 0.01$, * $P < 0.05$, ns = not
538 significant by one-way ANOVA with a Dunnett's (**D** and **F**) or Dunn's (**E** and **G**) post-test). (**B-G**)
539 Bars indicate the geometric mean values, and dotted lines are the LOD of the assays. The
540 results are from one experiment, and each symbol represents an individual animal.

541 **STAR METHODS**

542 **RESOURCE AVAILABILITY**

543 **Lead contact.** Further information and requests for resources and reagents should be
544 directed to the Lead Contact, Adrianus C.M. Boon (jboon@wustl.edu).

545 **Materials availability.** All requests for resources and reagents should be directed to the
546 Lead Contact author. This includes viruses, vaccines, and primer-probe sets. All reagents will
547 be made available on request after completion of a Materials Transfer Agreement.

548 **Data and code availability.** All data supporting the findings of this study are available
549 within the paper and are available from the corresponding author upon request. This paper does
550 not include original code. Any additional information required to reanalyze the data reported in
551 this paper is available from the lead contact upon request.

552

553 **EXPERIMENTAL MODEL AND SUBJECT DETAILS**

554 **Cells and Viruses.** Vero cells expressing human ACE2 and TMPRSS2 (Vero-hACE2-
555 hTMPRSS2 [6, 35], gift from Adrian Creanga and Barney Graham, NIH) were cultured at 37°C
556 in Dulbecco's Modified Eagle medium (DMEM) supplemented with 10% fetal bovine serum
557 (FBS), 10 mM HEPES (pH 7.3), 100 U/mL of Penicillin-Streptomycin, and 10 µg/mL of
558 puromycin. Vero cells expressing TMPRSS2 (Vero-hTMPRSS2) [35] were cultured at 37°C in
559 Dulbecco's Modified Eagle medium (DMEM) supplemented with 10% fetal bovine serum (FBS),
560 10 mM HEPES (pH 7.3), 100 U/mL of Penicillin-Streptomycin, and 5 µg/mL of blasticidin.

561 SARS-CoV-2 (strain 2019-nCoV/USA-WA1/2020) was obtained from the US Centers for
562 Disease Control (CDC) and propagated on Vero-hTMPRSS2 cells. The B.1.621 variant of
563 SARS-CoV-2 (strain hCoV-19/USA/WI-UW-4340/2021) was obtained from a nasal swab isolate
564 and propagated on Vero-hTMPRSS2 cells. Recombinant SARS-CoV-2 with a N501Y and
565 D614G mutations in the S protein of SARS-CoV-2 has been published previously [6] and was
566 propagated on Vero-hTMPRSS2 cells. The virus stocks were subjected to next-generation

567 sequencing, and the S protein sequences were identical to the original isolates. The infectious
568 virus titer was determined by plaque or focus-forming assay on Vero-hACE2-hTMPRSS2 or
569 Vero-hTMPRSS2 cells.

570 **Pre-clinical vaccine mRNA and lipid nanoparticle production process.** A sequence-
571 optimized mRNA encoding prefusion-stabilized Wuhan-Hu-1 (mRNA-1273) SARS-CoV-2 S-2P
572 protein was synthesized *in vitro* using an optimized T7 RNA polymerase-mediated transcription
573 reaction with complete replacement of uridine by N1m-pseudouridine [36]. The reaction included
574 a DNA template containing the immunogen open-reading frame flanked by 5' untranslated
575 region (UTR) and 3' UTR sequences and was terminated by an encoded polyA tail. After
576 transcription, the cap-1 structure was added to the 5' end using the vaccinia virus capping
577 enzyme (New England Biolabs) and vaccinia virus 2'-O-methyltransferase (New England
578 Biolabs). The mRNA was purified by oligo-dT affinity purification, buffer exchanged by tangential
579 flow filtration into sodium acetate, pH 5.0, sterile filtered, and kept frozen at -20°C until further
580 use.

581 The mRNA was encapsulated in a lipid nanoparticle through a modified ethanol-drop
582 nanoprecipitation process described previously [37]. Ionizable, structural, helper, and
583 polyethylene glycol lipids were briefly mixed with mRNA in an acetate buffer, pH 5.0, at a ratio of
584 2.5:1 (lipid:mRNA). The mixture was neutralized with Tris-HCl, pH 7.5, sucrose was added as a
585 cryoprotectant, and the final solution was sterile-filtered. Vials were filled with formulated lipid
586 nanoparticle and stored frozen at -20°C until further use. The vaccine product underwent
587 analytical characterization, which included the determination of particle size and polydispersity,
588 encapsulation, mRNA purity, double-stranded RNA content, osmolality, pH, endotoxin, and
589 bioburden, and the material was deemed acceptable for *in vivo* study.

590 **Recombinant proteins.** Recombinant S, was expressed as previously described [38].
591 Briefly, a mammalian cell codon-optimized nucleotide sequence coding for soluble S (GenBank:
592 MN908947.3, amino acids 1-1,213) modified to remove the polybasic cleavage site (RRAR to

593 A), but introducing two stabilizing mutations (K986P and V987P, wild-type numbering) and a C-
594 terminal thrombin cleavage site, T4 foldon trimerization domain, and a 6xHIS tag were cloned
595 into mammalian expression vector pCAGGS [39]. Recombinant S was produced in Expi293F
596 cells (ThermoFisher, Cat #A14527) by transfection with purified DNA using the ExpiFectamine
597 293 Transfection Kit (ThermoFisher, Cat #A14524). Supernatants from transfected cells were
598 harvested 4 days post-transfection, and recombinant proteins were purified using Ni-NTA
599 agarose (ThermoScientific, Cat #88222), then buffer exchanged into phosphate buffered saline
600 (PBS) and concentrated using Amicon Ultracel centrifugal filters (EMD Millipore, UFC903024).

601 **Mouse experiments.** Animal studies were carried out in accordance with the
602 recommendations in the Guide for the Care and Use of Laboratory Animals of the National
603 Institutes of Health. The protocols were approved by the Institutional Animal Care and Use
604 Committee at the Washington University School of Medicine (assurance number A3381-01).
605 Seven-to-nine week old male 129S2 (strain: 129S2/SvPasCrl, Cat # 287) or female K18-hACE2
606 transgenic mice (strain: 2B6.Cg-Tg(K18-ACE2)2Prlmn/J, Cat # 34860) were obtained from
607 Charles River Laboratories and Jackson Laboratories, respectively and housed at Washington
608 University. Animals were housed in groups and fed standard chow diet.

609 Some of the animals were vaccinated via intramuscular (IM) route with 10^8 , 10^9 , or 10^{10} viral
610 particles of fresh or freeze-thawed Ad26.COV2.S in 100 μ L of phosphate buffered saline (PBS).
611 The freeze-thawed vaccine was stored at -80°C prior to thawing at room temperature. No
612 difference in serum antibody responses were detected between the fresh and freeze-thawed
613 Ad26.COV2.S vaccine (**Fig S1A-B**). Control animals for the adenoviral vaccine received PBS
614 alone. Twenty-one days and 115 days later, serum samples were obtained, and used for ELISA
615 and virus neutralization assays. Separately, 129S2 mice and K18-hACE2 mice were immunized
616 and boosted with 0.25 or 5 μ g of mRNA-1273 or a control mRNA (mRNA-control) vaccine at
617 three week intervals. Twenty-one days after the second immunization, serum was obtained and
618 used for virus neutralization assays.

619 Following transfer to the enhanced Biosafety level 3 laboratory, the animals were challenged
620 via intranasal route with 10^3 or 10^5 PFU of the SARS-CoV-2 N501Y/D614G or B.1.621 variant.
621 Animal weights were measured daily for the duration of the experiment. At different time points
622 after challenge, the animals were sacrificed, and their lungs were collected for virological and
623 histological analysis. The left lobe was homogenized in 1.0 mL of Dulbecco's Modified Eagle
624 Medium (DMEM), clarified by centrifugation (1,000 x g for 5 min) and used for viral titer analysis
625 by quantitative RT-PCR (RT-qPCR) using primers and probes targeting the *N* gene, and by
626 plaque assay. A nasal wash also was collected, by inoculating 1.0 mL of PBS with 0.1% bovine
627 serum albumin into one nostril and collecting the wash from the other nostril (**Fig 1** and **4**).
628 Alternatively, 0.5 mL of PBS with 0.1% bovine serum albumin was flushed through the nasal
629 cavity after dissecting off the lower jaw (**Fig 2-3**). The nasal wash was clarified by centrifugation
630 (2,000 x g for 10 min) and used for viral titer analysis by RT-qPCR using primers and probes
631 targeting the *N* gene, and by plaque assay.

632 **Hamster experiments.** Animal studies were carried out in accordance with the
633 recommendations in the Guide for the Care and Use of Laboratory Animals of the National
634 Institutes of Health. The protocols were approved by the Institutional Animal Care and Use
635 Committee at the Washington University School of Medicine (assurance number A3381-01).
636 Five-week old male hamsters were obtained from Charles River Laboratories and housed at
637 Washington University. Five days after arrival, the animals were immunized via intramuscular
638 injection with 10^8 or 10^{10} viral particles of freeze-thawed Ad26.COV2.S in 100 μ L of PBS.
639 Control animals received PBS alone. Twenty-one days later, serum samples were obtained, and
640 the animals were transferred to the enhanced Biosafety level 3 laboratory. One day later, the
641 animals were challenged via intranasal route with 10^3 PFU of WA1/2020 or B.1.621 variant.
642 Animal weights were measured daily for the duration of the experiment. Four days after
643 challenge, the animals were sacrificed, and their lungs were collected for virological and
644 histological analysis. The left lobe was homogenized in 1.0 mL of DMEM, clarified by

645 centrifugation (1,000 x g for 5 min) and used for viral titer analysis by quantitative RT-PCR using
646 primers and probes targeting the *N* gene, and by plaque assay. A nasal wash was also
647 collected, by inoculating 1.0 mL of PBS with 0.1% bovine serum albumin into one nostril and
648 collecting the wash from the other nostril. The nasal wash was clarified by centrifugation (2,000
649 x g for 10 min) and used for viral titer analysis by quantitative RT-PCR using primers and probes
650 targeting the *N* gene, and by plaque assay.

651

652 **METHOD DETAILS**

653 **Focus reduction neutralization titer assay (FRNT).** Serial dilutions of serum samples
654 were incubated with 10^2 focus-forming units (FFU) of different strains of SARS-CoV-2 for 1 h at
655 37°C. Antibody-virus complexes were added to Vero-hTMPRSS2 cell monolayers in 96-well
656 plates and incubated at 37°C for 1 h. Subsequently, cells were overlaid with 1% (w/v)
657 methylcellulose in Eagle's Minimal Essential medium (MEM, Thermo Fisher Scientific). Plates
658 were harvested 30 h later by removing overlays and fixed with 4% paraformaldehyde (PFA) in
659 PBS for 20 min at room temperature. Plates were washed and sequentially incubated with an
660 oligoclonal pool of SARS2-2, SARS2-11, SARS2-16, SARS2-31, SARS2-38, SARS2-57, and
661 SARS2-71 [40] anti-S protein antibodies and HRP-conjugated goat anti-mouse IgG (Sigma Cat
662 # A8924) in PBS supplemented with 0.1% saponin and 0.1% bovine serum albumin. SARS-
663 CoV-2-infected cell foci were visualized using TrueBlue peroxidase substrate (KPL) and
664 quantitated on an ImmunoSpot microanalyzer (Cellular Technologies).

665 **Virus titration assays.** Plaque assays were performed on Vero-hACE2-hTRMPSS2 cells in
666 24-well plates. Lung tissue homogenates or nasal washes were diluted serially by 10-fold,
667 starting at 1:10, in cell infection medium (DMEM + 2% FBS + 100 U/mL of penicillin-
668 streptomycin). Two hundred and fifty microliters of the diluted virus were added to a single well
669 per dilution per sample. After 1 h at 37°C, the inoculum was aspirated, the cells were washed
670 with PBS, and a 1% methylcellulose overlay in MEM supplemented with 2% FBS was added.

671 Seventy-two hours after virus inoculation, the cells were fixed with 4% formalin, and the
672 monolayer was stained with crystal violet (0.5% w/v in 25% methanol in water) for 1 h at 20°C.
673 The number of plaques were counted and used to calculate the plaque forming units/mL
674 (PFU/mL).

675 To quantify viral load in lung tissue homogenates and nasal washes, RNA was extracted
676 from 100 µL samples using E.Z.N.A.[®] Total RNA Kit I (Omega) and eluted with 50 µL of water.
677 Four microliters RNA was used for real-time RT-qPCR to detect and quantify *N* gene of SARS-
678 CoV-2 using TaqMan™ RNA-to-CT 1-Step Kit (Thermo Fisher Scientific) as described [41]
679 using the following primers and probes: Forward: GACCCCAAATCAGCGAAAT; Reverse:
680 TCTGGTACTGCCAGTTGAATCTG; Probe: ACCCCGCATTACGTTTGGTGGACC;
681 5'Dye/3'Quencher: 6-FAM/ZEN/IBFQ. Viral RNA was expressed as *N* gene copy numbers per
682 mg for lung tissue homogenates or mL for nasal swabs and nasal washes, based on a standard
683 included in the assay, which was created via *in vitro* transcription of a synthetic DNA molecule
684 containing the target region of the *N* gene.

685 **Histology.** The lungs from SARS-CoV-2 infected and control mice and hamsters were fixed
686 in 10% formalin for seven days. Lungs were embedded in paraffin and sectioned before
687 hematoxylin and eosin staining. Lung slides were scanned using the Hamamatsu NanoZoomer
688 slide scanning system and head sections were imaged using the Zeiss AxioImager Z2 system.

689 **ELISA.** Ninety-six-well microtiter plates (Nunc MaxiSorp; ThermoFisher Scientific) were
690 coated with 100 µL of recombinant SARS-CoV-2 S protein (Wuhan strain) at a concentration of
691 1 µg/mL in PBS (Gibco) at 4 °C overnight; negative control wells were coated with 1 µg/mL of
692 BSA (Sigma). Plates were blocked for 1.5 h at room temperature with 280 µL of blocking
693 solution (PBS supplemented with 0.05% Tween-20 (Sigma) and 10% FBS (Corning)). Serum
694 from mice and hamsters were diluted serially in blocking solution, starting at 1:100 dilution and
695 incubated for 1.5 h at room temperature. The plates were washed three times with T-PBS (1X
696 PBS supplemented with 0.05% Tween-20), and 100 µL of goat anti-mouse IgG (Southern

697 Biotech Cat #1030-05) diluted 1:2,000 in blocking solution or 100 μ L of HRP-conjugated anti-
698 hamster IgG(H+L) antibody (Southern Biotech Cat. #6061-05) diluted 1:500 in blocking solution,
699 was added to all wells and incubated for 1 h at room temperature. Plates were washed 3 times
700 with T-PBS and 3 times with 1X PBS, and 100 μ L of 1-step Ultra TMB-ELISA substrate solution
701 (Thermo Fisher Scientific) was added to all wells. The reaction was stopped after 5 min using
702 100 μ L of 1M HCl, and the plates were analyzed at a wavelength of 490 nm using a microtiter
703 plate reader (BioTek).

704

705 **QUANTIFICATION AND STATISTICAL ANALYSES**

706 Statistical significance was assigned when *P* values were < 0.05 using GraphPad Prism version
707 9.3. Tests, number of animals, median values, and statistical comparison groups are indicated
708 in the Figure legends. Analysis of weight change was determined by two-way ANOVA. Changes
709 in infectious virus titer, viral RNA levels, or serum antibody responses were compared to
710 unvaccinated or mRNA-control immunized animals and were analyzed by one-way ANOVA with
711 a multiple comparisons correction, unpaired t-test, or Mann-Whitney test, dependent on the
712 number of comparison and the distribution of the data.

713 **SUPPLEMENTARY FIGURE LEGENDS**

714 **Figure S1. Effect of an additional freeze-thaw on the immunogenicity of the**
715 **Ad26.COV2.S vaccine, Related to Fig 1. (A)** Neutralizing titer (IC_{50}) against WA1/2020
716 N501Y/D614G of serum obtained from 129S2 mice immunized once with 10^8 (red symbols), 10^9
717 (purple symbols), or 10^{10} (blue symbols) of fresh (solid symbols) or freeze-thawed (open
718 symbols) Ad26.COV2.S. (ns = not significant by unpaired t-test). **(B)** Serum anti-S protein
719 antibody response (EC_{50}) in control mice (black symbols), and mice immunized with 10^8 (red
720 symbols), 10^9 (purple symbols), or 10^{10} (blue symbols) of fresh or freeze-thawed Ad26.COV2.S
721 (ns = not significant by unpaired t-test). **(C)** Serum anti-S protein specific antibody response
722 (EC_{50}) in mice 21 and 115 days after immunization with 10^8 (red symbols), 10^9 (purple symbols),
723 or 10^{10} (blue symbols) of fresh or freeze-thawed Ad26.COV2.S. Each symbol represents an
724 individual animal.

725 **Figure S2. Serum neutralization titer of the B.1.621 variant by sera from immunized**
726 **mice and Syrian hamsters against, Related to Fig 1-4. (A)** Pairwise comparison of the
727 neutralizing titer (IC_{50}) against WA1/2020 N501Y/D614G and B.1.621 for individual sera
728 obtained from 129S2 mice immunized once with 10^8 (red symbols), 10^9 (purple symbols), or 10^{10}
729 (blue symbols) of fresh (solid symbols) or freeze-thawed (open symbols) Ad26.COV2.S. (ns =
730 not significant by paired t-test). **(B)** Pairwise comparison of the neutralizing titer (IC_{50}) against
731 WA1/2020 N501Y/D614G and B.1.621 for individual sera obtained from K18-hACE2 mice
732 immunized twice with 0.25 μ g (open symbols) or 5 μ g (closed symbols) of mRNA1273 vaccine.
733 (** $P < 0.01$, * $P < 0.05$ by paired t-test). **(C)** Pairwise comparison of the neutralizing titer (IC_{50})
734 against WA1/2020 N501Y/D614G and B.1.621 for individual sera obtained from 129/S2 mice
735 immunized twice with 0.25 μ g (open symbols) or 5 μ g (closed symbols) of mRNA1273 vaccine.
736 (ns = not significant by paired t-test). **(D)** Pairwise comparison of the neutralizing titer (IC_{50})
737 against WA1/2020 and B.1.621 for individual sera obtained from Syrian hamsters immunized
738 once with 10^8 (red symbols) or 10^{10} (blue symbols) of fresh (solid symbols) or freeze-thawed

739 (open symbols) Ad26.COVS.S. (**** $P < 0.0001$, *** $P < 0.001$, by paired t-test). Each symbols
740 is an individual animal.

741 **Figure S3. Histological analysis of lung tissue sections from mRNA-1273 and mRNA-**
742 **control immunized and K18-hACE2 mice challenged with WA1/2020 N501Y/D614G or**
743 **B.1.621, Related to Fig 2.** Representative images of 50x, 200x and 400x magnification of
744 hematoxylin and eosin staining of lung sections from K18-hACE2 mice immunized with 0.25 μ g
745 (A) and 5 μ g (B) of mRNA-1273 or an mRNA-control (mRNA-CTRL) vaccine and challenged 64
746 days later with WA1/2020 N501Y/D614G or B.1.621. (C) A mock infection is included as a
747 control. Lungs were collected 7 days post challenge, fixed in 10% formalin and paraffin
748 embedded prior to sectioning and staining. The scale bar is 1 mm, 0.25mm and 0.1mm for 50x,
749 200x and 400x respectively. Representative images are shown from $n = 2$ per group.

750 **Figure S4. Histological analysis of lung tissue sections from mRNA-1273 and mRNA-**
751 **control immunized 129S2 mice challenged with WA1/2020 N501Y/D614G or B.1.621,**
752 **Related to Fig 3.** Representative images at 50x, 200x and 400x magnification of hematoxylin
753 and eosin staining of lung sections from 129S2 mice immunized with 0.25 μ g (A) and 5 μ g (B)
754 of mRNA-1273 or an mRNA-control (mRNA-CTRL) vaccine and challenged 62 days later with
755 WA1/2020 N501Y/D614G or B.1.621 virus. (C) A mock infection is included as a control. Lungs
756 were collected 4 days post challenge, fixed in 10% formalin and paraffin embedded prior to
757 sectioning and staining. The scale bar is 1 mm, 0.25mm and 0.1mm for 50x, 200x and 400x
758 respectively. Representative images are shown from $n = 2$ per group.

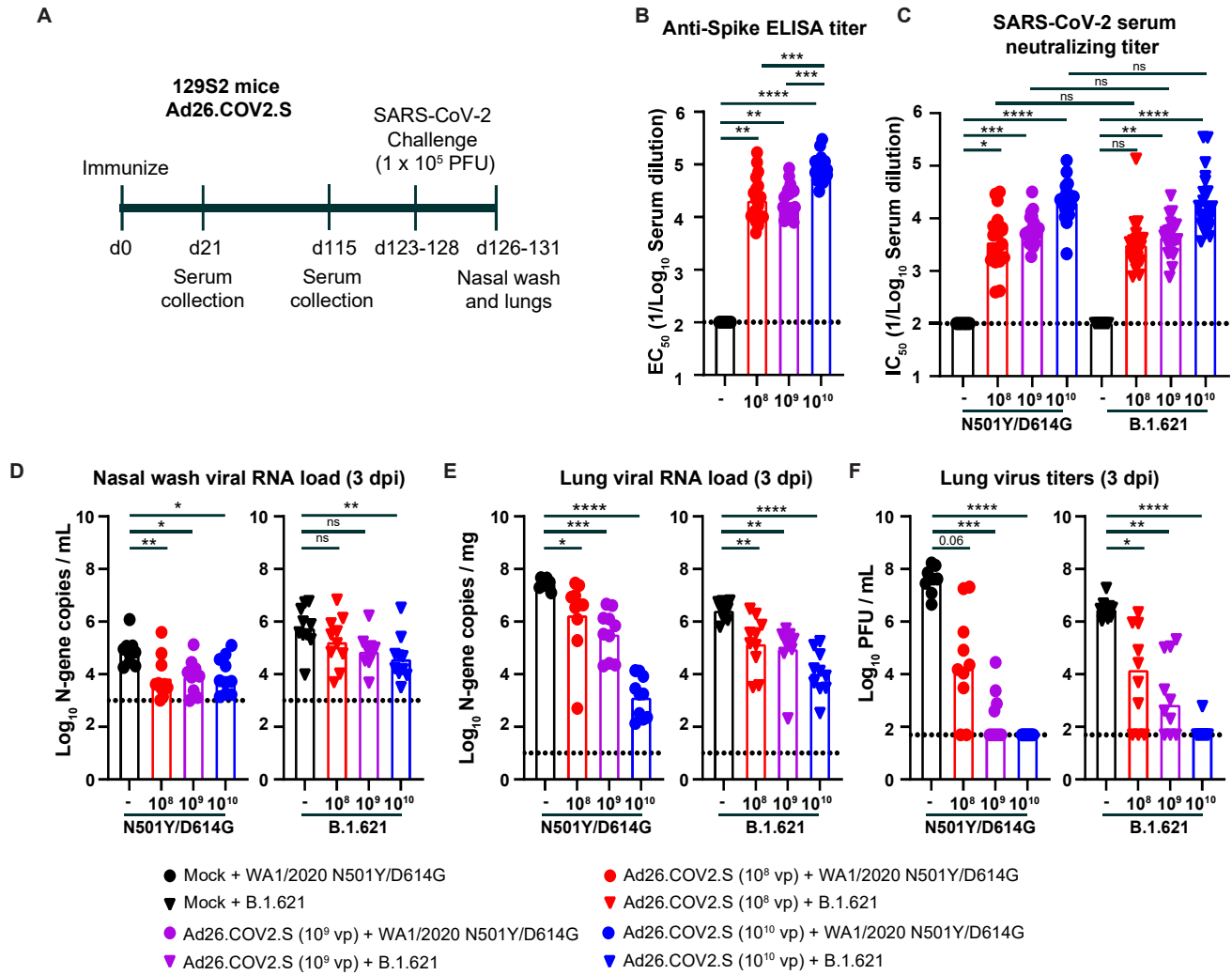


Figure 1

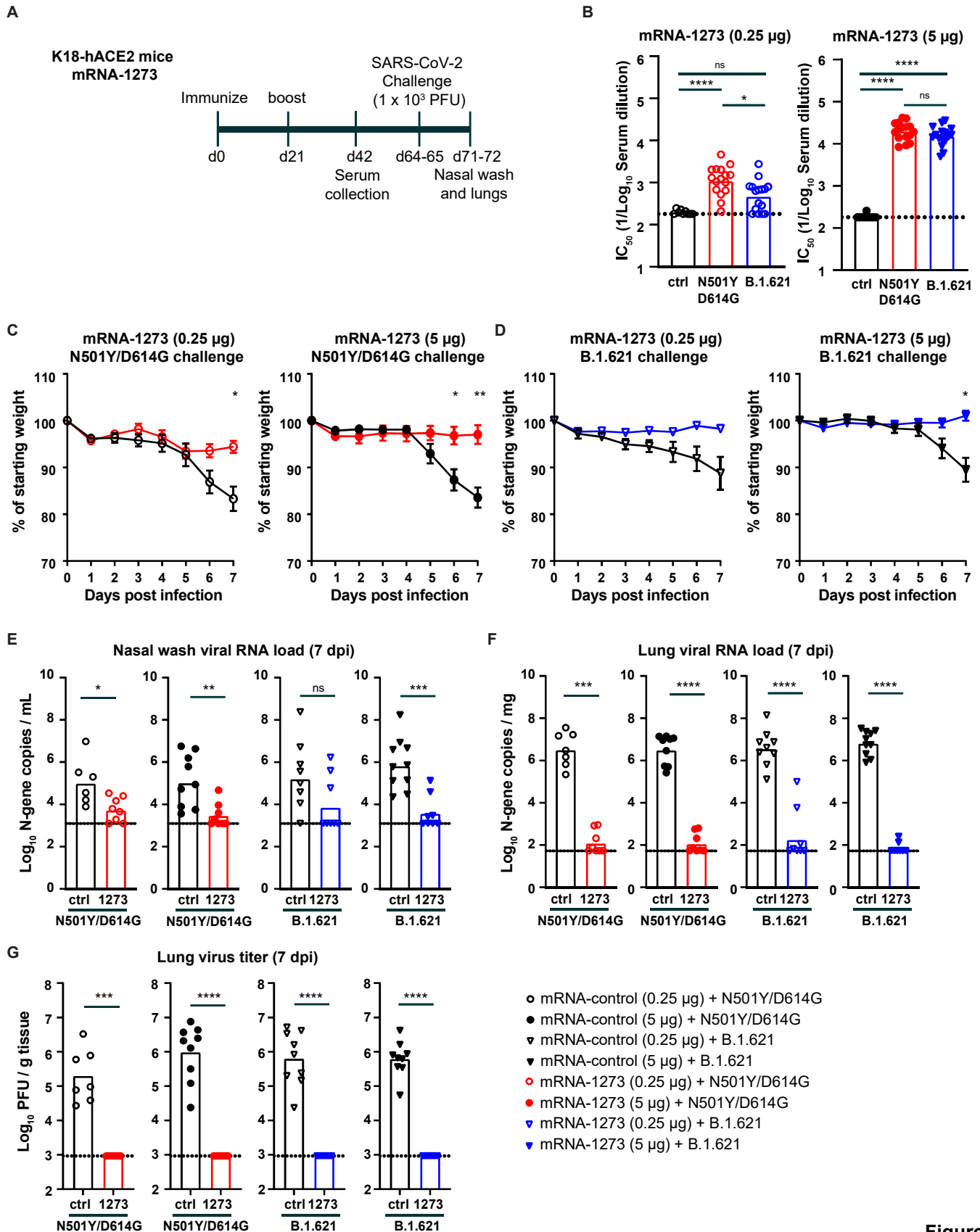


Figure 2

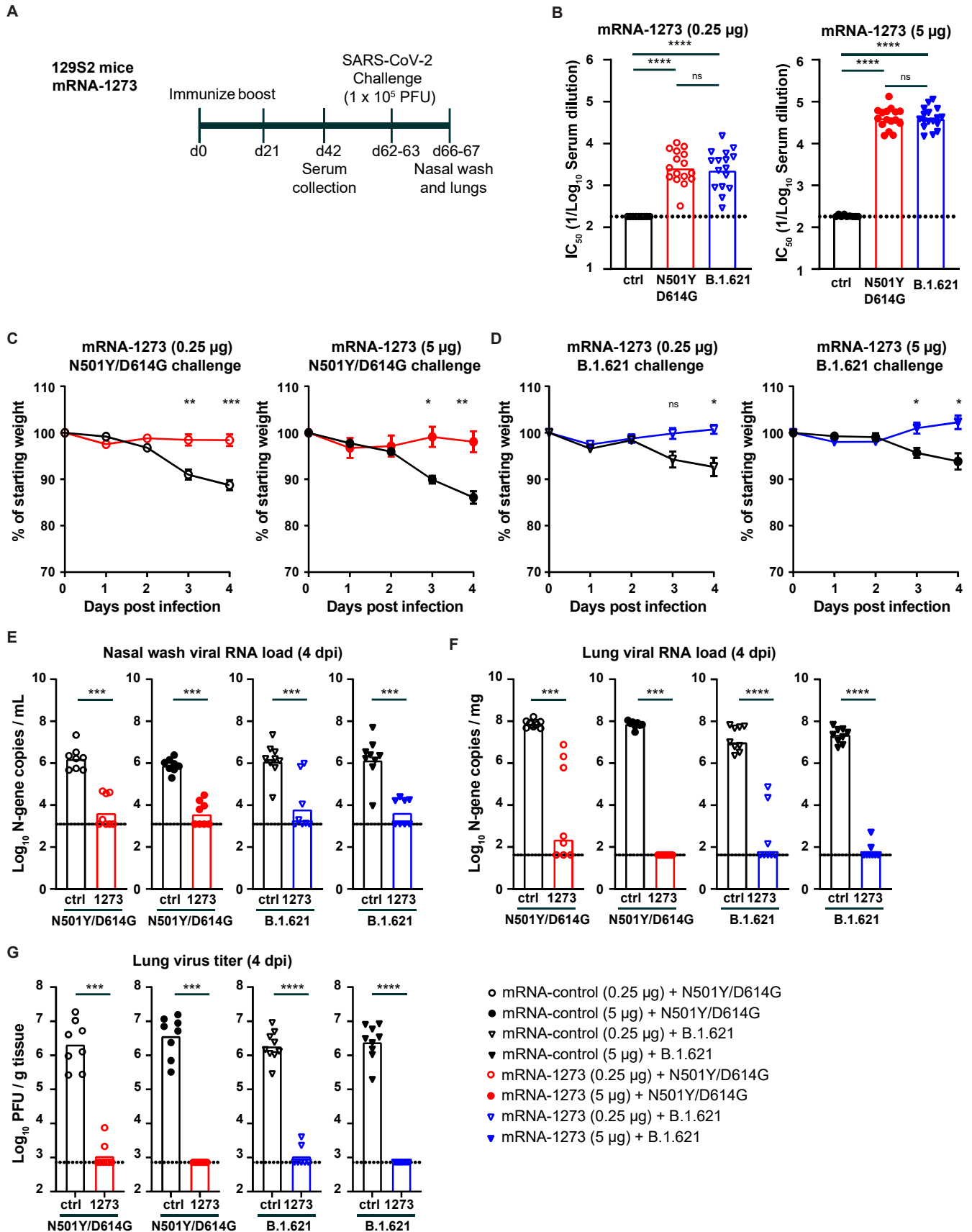


Figure 3

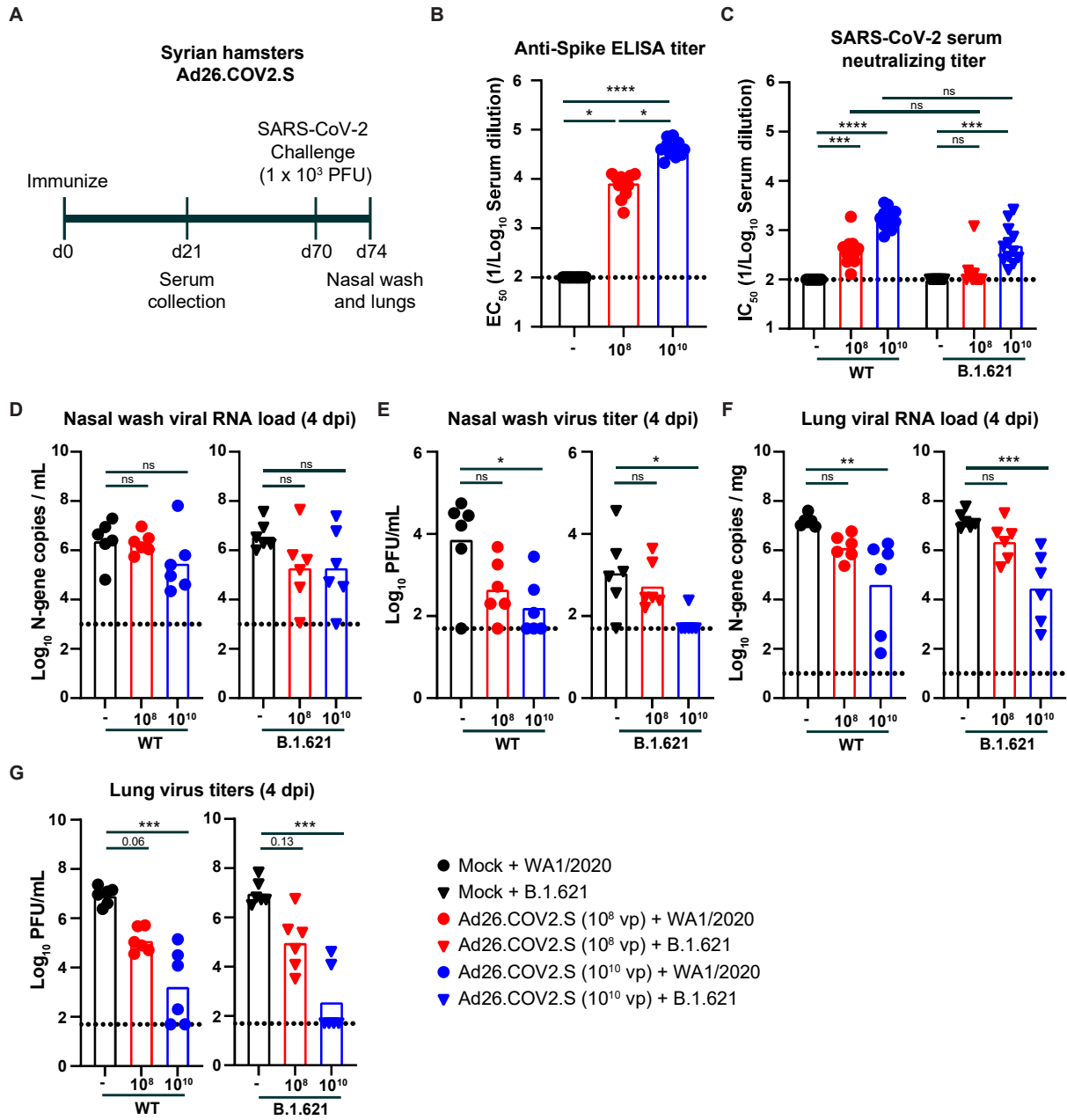


Figure 4